Out-of-Distribution Generalization with a SPARC: Racing 100 Unseen Vehicles with a Single Policy

Bram Grooten^{1,2} Patrick MacAlpine¹ Kaushik Subramanian¹ Peter Stone^{1,3} Peter R. Wurman¹

¹Sony AI ²TU Eindhoven ³The University of Texas at Austin

Abstract

Generalization to unseen environments is a significant challenge in the field of robotics and control. In this work, we focus on contextual reinforcement learning, where agents act within environments with varying contexts, such as selfdriving cars or quadrupedal robots that need to operate in different terrains or weather conditions than they were trained for. We tackle the critical task of generalizing to out-ofdistribution (OOD) settings, without access to explicit context information at test time. Recent work has addressed this problem by training a context encoder and a history adaptation module in separate stages. While promising, this two-phase approach is cumbersome to implement and train. We simplify the methodology and introduce SPARC: single-phase adaptation for robust control. We test SPARC on varying contexts within the high-fidelity racing simulator Gran Turismo 7 and wind-perturbed MuJoCo environments, and find that it achieves reliable and robust OOD generalization.

Code — https://github.com/bramgrooten/sparc

1 Introduction

Deep reinforcement learning (RL) has demonstrated successful performance in fields such as robotics (Mahmood et al. 2018), nuclear fusion (Degrave et al. 2022), and high-fidelity racing simulators (Wurman et al. 2022). Despite these successes, generalizing RL agents to unseen environments with varying contextual factors remains a critical challenge. In real-world applications, environmental conditions such as friction, wind speed, or vehicle dynamics can change unpredictably, often leading to catastrophic failures when the agent encounters out-of-distribution (OOD) contexts that it was not trained for.

A promising approach to tackle this issue is context-adaptive reinforcement learning (Benjamins et al. 2021), where agents infer and adapt to latent environmental factors by leveraging past interactions. Rapid Motor Adaptation (RMA) (Kumar et al. 2021) is a notable framework in this direction, introducing a two-phase learning procedure. In the first phase, a context encoder is trained using privileged information about the environment. The second phase then employs supervised learning to train a history-based

Copyright © 2026, Association for the Advancement of Artificial Intelligence (www.aaai.org). All rights reserved.

adaptation module, enabling the agent to infer latent context solely from past state-action trajectories. While effective, this two-phase approach introduces complexity during implementation and training.

In this work, we introduce **SPARC** (single-phase adaptation for robust control), a novel algorithm that unifies context encoding and adaptation into a single training phase, as illustrated in Figure 1. SPARC is straightforward to implement and naturally integrates with off-policy training as well as asynchronous distributed computation on cloud-based rollout workers. Algorithms such as SPARC and RMA are advantageous when explicit context labels are unavailable at test time, a frequent limitation in real-world robotic deployment. By collapsing adaptation into a single training loop, SPARC is naturally compatible with on-device continual learning—especially applicable in settings where retraining in the cloud is prohibitive due to privacy or latency constraints. In contrast, RMA is unable to perform continual learning in a straightforward manner.

We evaluate SPARC on two distinct domains: (1) a set of *MuJoCo* environments featuring strongly varying environment dynamics through the use of wind perturbations, and (2) a high-fidelity racing simulator, *Gran Turismo 7*, where agents must adapt to different car models on multiple tracks. SPARC achieves state-of-the-art generalization performance and consistently produces Pareto-optimal policies when evaluated across multiple desiderata.

Our contributions are summarized as follows.

- We introduce SPARC, a novel single-phase training method for context-adaptive reinforcement learning, eliminating the need for separate encoder pre-training.
- We empirically validate SPARC's generalization ability across OOD environments, demonstrating competitive or superior performance compared to existing approaches.
- We perform and analyze several ablation studies, examining key design choices such as history length and the selection of rollout policy during training.

2 Related Work

Generalization to out-of-distribution environments is a fundamental challenge in reinforcement learning, hindering its deployment in real-world applications, particularly in robotics and control tasks (Kirk et al. 2023). The learning

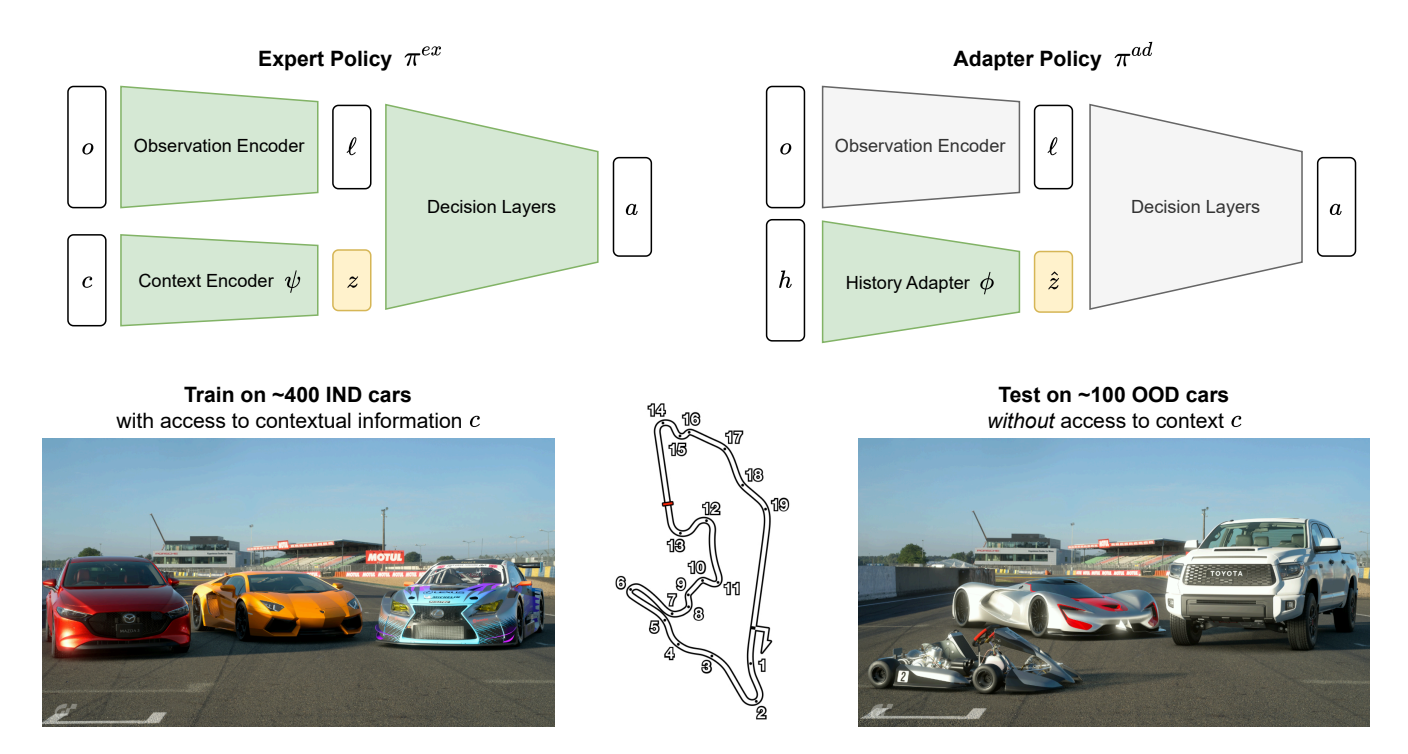


Figure 1: Overview of our algorithm SPARC (top) and the problem setting in Gran Turismo 7 (bottom). SPARC trains an expert policy π^{ex} and an adapter policy π^{ad} simultaneously in a single phase. The adapter policy does not require access to privileged contextual information, facilitating deployment to OOD real-world scenarios. Observations o, contextual information c, and a history of recent observation-action pairs h are passed into the networks. Latent encodings ℓ and z are concatenated and passed to the final layers, producing action a. Similar to RMA (Kumar et al. 2021), π^{ex} is trained with reinforcement learning, while the History Adapter ϕ of π^{ad} is trained with supervised learning to regress its encoding $\phi(h) = \hat{z}$ to the Context Encoder's output $\psi(c) = z$. Note that since SPARC trains in one phase, the context encoding z is a moving target, instead of a traditionally fixed target in RMA. Trainable modules are in green. The black modules regularly copy weights from their counterpart in π^{ex} .

dynamics of RL methods often struggle to adapt to novel environmental conditions (Lyle et al. 2022). Contextual reinforcement learning (Langford 2017; Benjamins et al. 2021) provides a framework to address this problem by training agents capable of adapting to varying environmental factors.

2.1 Contextual RL

Robust RL often depends on effective contextual adaptation. Recent work has explored context-aware policies that integrate contextual cues into decision-making (Beukman et al. 2023; Chen et al. 2021; Lahmer et al. 2024) or employ world models to capture environment dynamics (Lee et al. 2020b; Prasanna et al. 2024). In addition, several studies have focused on modifying the environment itself—such as by varying gravity or adjusting agent component dimensions—to promote the development of more versatile controllers (Benjamins et al. 2021; Leon et al. 2024).

2.2 What if the Agent has No Access to Context?

In many real-world scenarios, agents are deprived of explicit contextual information during deployment. In these cases, the agent must infer the relevant environmental factors indirectly. For instance, Lee et al. (2020a) advanced robust legged locomotion by introducing a two-phase learn-

ing process. It first trains an expert policy, which includes a context encoder using the privileged contextual information. The second phase involves an adapter policy that tries to imitate the expert's action, while a history-based adaptation component aims to minimize the difference between its history encoding and the expert's context encoding. Rapid Motor Adaptation (Kumar et al. 2021) refines this methodology by only imitating the context encoding, not the action. The adapter policy can be deployed, as it does not require access to the privileged context.

2.3 Other Techniques for Generalization

Several complementary approaches have been proposed to enhance generalization. Domain randomization (Tobin et al. 2017; Peng et al. 2018) and procedurally generated environments (Cobbe et al. 2020; Gisslén et al. 2021) introduce diversity during training, thereby encouraging robust policy behavior. We employ domain randomization by default in our experiments. System identification methods (Yu et al. 2017)—whether performed explicitly or through implicit online adaptation, as in SPARC and RMA—also contribute to improved performance under varying conditions. Moreover, techniques such as data augmentation (Laskin et al. 2020; Hansen, Su, and Wang 2021; Wang et al. 2024)

and masking (Grooten et al. 2024; Huang et al. 2022) have been shown to further enhance generalization, particularly for pixel-based inputs.

Meta-reinforcement learning offers an alternative paradigm for learning adaptable policies (Wang et al. 2016; Rabinowitz et al. 2018; Duan et al. 2016). Foundational algorithms like Model-Agnostic Meta-Learning (MAML) (Finn, Abbeel, and Levine 2017) enable rapid task adaptation, and emerging methods using hypernetworks generate task-specific policy parameters on the fly (Beck et al. 2023; Rezaei-Shoshtari et al. 2023; Beukman et al. 2023).

3 Background

In this section, we formalize the underlying problem framework and examine the core techniques that form the foundation for SPARC, enabling context-adaptive behavior.

3.1 Problem Formulation

We consider a contextual Markov decision process (CMDP) (Hallak, Di Castro, and Mannor 2015; Abbasi-Yadkori and Neu 2014), defined by Kirk et al. (2023) as a tuple $\mathcal{M} = (\mathcal{S}, \mathcal{A}, \mathcal{O}, \mathcal{C}, R, T, O, p_s, p_c)$ where:

- S is the state space,
- A is the action space,
- \mathcal{O} is the observation space,
- C is the context space,
- $R: \mathcal{S} \times \mathcal{A} \times \mathcal{C} \to \mathbb{R}$ is the reward function,
- $T: \mathcal{S} \times \mathcal{A} \times \mathcal{C} \to \Delta(\mathcal{S})$ defines the stochastic transition dynamics conditioned on a context $c \in \mathcal{C}$,
- $O: \mathcal{S} \times \mathcal{C} \to \mathcal{O}$ is the observation function,
- $p_s: \mathcal{C} \to \Delta(\mathcal{S})$ is the distribution over initial states s_0 given a context $c \in \mathcal{C}$, and
- $p_c \in \Delta(\mathcal{C})$ is the distribution over contexts.

During training, the agent will be exposed to a certain subset of contexts $\mathcal{C}_{\text{IND}} \subset \mathcal{C}$, which are in-distribution (IND), short for within the training distribution. To test generalization ability, we hold out a different subset of contexts $\mathcal{C}_{\text{OOD}} \subset \mathcal{C}$ that are out-of-distribution (OOD). We ensure that there is no overlap: $\mathcal{C}_{\text{IND}} \cap \mathcal{C}_{\text{OOD}} = \varnothing$. This separation defines two sub-CMDPs: \mathcal{M}_{IND} and \mathcal{M}_{OOD} . We specify the context distributions to be uniform over their respective subsets:

$$p_c^i(c) = \begin{cases} \frac{1}{|\mathcal{C}_i|} & \text{if } c \in \mathcal{C}_i\\ 0 & \text{otherwise,} \end{cases}$$
 (1)

for $i \in \{\text{IND}, \text{OOD}\}.$

In our setting, the agents do not observe c at test time and must infer it through other means, for example from their interaction history. However, for comparison, we will also present results of an expert policy that does have access to the privileged context information $c \in \mathcal{C}_{\text{OOD}}$ at evaluation.

Our objective is to train a policy π that maximizes expected return across both in-distribution and out-of-distribution contexts, while only having access to privileged contextual information $c \in \mathcal{C}_{\text{IND}}$ during training.

3.2 Pure History-based Policies

History-based policies have emerged as a powerful approach in reinforcement learning for inferring hidden environmental context from past interactions. Instead of relying solely on the current observation $o_t \in \mathcal{O}$, these policies condition action selection on a sequence of recent observation-action pairs. Let H be the history length and $\mathcal{H} = (\mathcal{O} \times \mathcal{A})^H$, the space of possible histories. For time t we define the corresponding history h_t as

$$h_t = (o_{t-H:t-1}, a_{t-H:t-1}) \in \mathcal{H}.$$

This history input results in policies of the form $\pi:\mathcal{O}\times\mathcal{H}\to\Delta(\mathcal{A})$. Including the history may enable the agent to implicitly capture latent context information $c\in\mathcal{C}$, as the context c may influence the environment dynamics.

A pure history-based approach is presented by Lee et al. (2020a) as a strong baseline. In their work on quadrupedal locomotion over challenging terrains, the authors demonstrate that leveraging an extended history of proprioceptive data via a temporal convolutional network (TCN) enables robust control in diverse settings.

4 Method

4.1 Leveraging Contextual Information

Training with privileged contextual information—even if not available at test time—has been shown to be particularly useful for generalizing to OOD contexts. In that regard, the approaches by Lee et al. (2020a) and Kumar et al. (2021) are almost equivalent; we will focus on Rapid Motor Adaptation (RMA) (Kumar et al. 2021). In RMA, two policies are trained in separate phases. First, the expert policy

$$\pi_{\theta}^{ex}: \mathcal{O} \times \mathcal{C} \to \Delta(\mathcal{A})$$

which includes a context encoder $\psi(\cdot)$ with access to the environment's privileged information, is trained using a reinforcement learning algorithm. While the original RMA work uses PPO (Schulman et al. 2017), we employ the more sample-efficient QR-SAC, proven to work well in Gran Turismo (Wurman et al. 2022).

Once training of π_{θ}^{ex} has converged to a sufficient level, the best model checkpoint π_{θ}^{ex} needs to be determined. This selection requires careful evaluation across multiple dimensions (Morrill et al. 2023), a cumbersome intermediate step that SPARC skips, as it is trained in a single phase.

The second stage of RMA trains the adapter policy

$$\pi_{\theta}^{ad}: \mathcal{O} \times \mathcal{H} \to \Delta(\mathcal{A})$$

while keeping the expert policy $\pi_{\theta^*}^{ex}$ frozen. In the adapter policy, a history adapter ϕ_{θ} processes a sequence of recent observation-action pairs h_t to produce a latent representation $\hat{z}_t = \phi_{\theta}(h_t)$. The history adapter is trained by minimizing the distance between $\hat{z}_t = \phi_{\theta}(h_t)$ and $z_t = \psi_{\theta^*}(c_t)$ through the mean squared error loss:

$$\mathcal{L}_{\phi}(c_t, h_t) = \mathbb{E}_{c_t, h_t}[(z_t - \hat{z}_t)^2]. \tag{2}$$

The history-inferred latent context \hat{z}_t is integrated into the policy. By conditioning on both the current observation o_t and the latent context \hat{z}_t , the policy can adjust its behavior to handle unseen or varying environmental conditions.

Table 1: Performance summary on IND and OOD settings across all test tracks in Gran Turismo, averaged over 3 seeds. Results show the mean built-in AI (BIAI) ratio across cars (ratio = the RL agent's lap time divided by the BIAI lap time, lower is better). If an algorithm fails to complete a lap with a specific vehicle, it receives a BIAI ratio of 2.0 for that car model. Additionally, we show the percentage of cars with a successfully completed lap (\pm s.e.m.). We **bold** the best out-of-distribution results across algorithms without access to context at test time (all except Oracle, see Table 3). We include IND results for reference. SPARC achieves the fastest OOD lap times on 2 of 3 tracks and completes the most laps with OOD vehicles overall.

Race Track	Method	IND		OOD	
ruce Truck	Welloa	BIAI ratio (↓)	Success % (†)	BIAI ratio (↓)	Success % (†)
Grand Valley	Only Obs History Input RMA	$\begin{array}{c} 0.9929 \pm 0.0007 \\ 0.9904 \pm 0.0001 \\ 1.0046 \pm 0.0054 \end{array}$	100.00 ± 0.00 99.68 ± 0.08 99.84 ± 0.16	$\begin{array}{c} 1.0641 \pm 0.0058 \\ 1.0826 \pm 0.0203 \\ 1.0560 \pm 0.0134 \end{array}$	$\begin{array}{c} 95.15 \pm 0.56 \\ 92.56 \pm 2.12 \\ 97.09 \pm 1.12 \end{array}$
	SPARC Oracle	0.9999 ± 0.0061 0.9884 ± 0.0005	99.76 ± 0.14 100.00 ± 0.00	$ 1.0491 \pm 0.0055 1.1348 \pm 0.0137 $	98.06 ± 0.56 90.94 ± 2.27
Nürburgring	Only Obs History Input RMA SPARC	1.0202 ± 0.0163 0.9984 ± 0.0030 1.1085 ± 0.0195 1.0254 ± 0.0061	95.87 ± 1.48 97.49 ± 0.32 88.03 ± 1.76 95.87 ± 0.49	1.1745 ± 0.0129 1.1204 ± 0.0132 1.2995 ± 0.0306 1.1199 ± 0.0076	81.88 ± 1.17 86.73 ± 1.29 77.99 ± 3.19 89.00 ± 0.86
	Oracle	0.9804 ± 0.0027	99.27 ± 0.28	1.1182 ± 0.0076 1.1182 ± 0.0215	89.64 ± 2.53
Catalunya Rallycross	Only Obs History Input RMA SPARC Oracle	0.9319 ± 0.0009 0.9294 ± 0.0001 0.9445 ± 0.0010 0.9432 ± 0.0027 0.9282 ± 0.0001	100.00 ± 0.00 100.00 ± 0.00 99.82 ± 0.18 100.00 ± 0.00 100.00 ± 0.00	0.9560 ± 0.0006 0.9553 ± 0.0068 0.9667 ± 0.0030 0.9631 ± 0.0026 1.1354 ± 0.0595	100.00 ± 0.00 99.33 ± 0.67 100.00 ± 0.00 100.00 ± 0.00 85.33 ± 5.81

4.2 Single-Phase Adaptation

Our algorithm illustrated in Figure 1, SPARC, greatly simplifies the implementation and training of agents capable of generalizing to out-of-distribution environments without access to privileged contextual information. In SPARC, the expert policy π^{ex} and the adapter policy π^{ad} are trained simultaneously, in contrast to the two-phase approach of RMA. This means that the context encoding $\psi(c)=z$ is a non-stationary target for the history adapter ϕ , instead of a fixed target. The results in Section 6 demonstrate that the adapter policy is able to manage these new learning dynamics.

An important detail in RMA is which model acts in the environment to collect experience. Policy π^{ex} acts in the first training phase, while π^{ad} does so in the second. This raises the question which policy should gather experience for SPARC, as both are trained together. One option would be to let the expert policy π^{ex} control the actions, since it is updated and improved through QR-SAC.

However, the expert policy, π^{ex} , is not the goal of the SPARC approach. A robust adapter policy, π^{ad} , is the overall learning target and using this policy to gather experience allows the learning algorithm to correct for any inaccuracies before final deployment. This brings the learning dynamics of π^{ad} closer to an on-policy setting, even though its history adapter ϕ is trained through supervised learning as shown in Equation 2. We perform an ablation study on this choice of rollout policy in the supplementary material.

SPARC's critic networks—necessary to run QR-SAC on π^{ex} —have the same architecture as the expert policy and thus have access to the context c. We can still run inference without knowing c, because at test time only π^{ad} is needed.

Reducing training of SPARC to one phase provides several benefits: (i) no intermediate selection of the best model checkpoint of the first phase is necessary, (ii) training can be easily continued indefinitely, without having to retrain the second phase, (iii) the simpler implementation facilitates the use of SPARC on asynchronous distributed systems.

5 Experimental Setup

In this section, we describe the experimental setup used to evaluate SPARC, our proposed single-phase adaptation method, in comparison with several baselines.

5.1 Environments

We evaluate our approach on two distinct domains:

- **MuJoCo:** A suite of continuous control tasks including *HalfCheetah*, *Hopper*, and *Walker2d* (Todorov, Erez, and Tassa 2012). We induce contextual variability by perturbing the environment's wind speed in multiple dimensions and scales, creating challenging OOD scenarios.
- **Gran Turismo 7:** A high-fidelity racing simulator that features diverse car models and realistic vehicle-track dynamics (Wurman et al. 2022). The simulator's rich contextual variability makes it an ideal testbed for assessing generalization to unseen conditions.

Within Gran Turismo, we experiment on two settings: (1) generalization across car models, and (2) generalization across differing engine power and vehicle mass settings for one specific car. The in-distribution (IND) training set and OOD test set are selected as follows:

Table 2: The Gran Turismo tracks which we experiment on in the *Car Models* setting. The road type and track length pose varying challenges.

Track	Length	Road Type
Grand Valley Nürburgring Catalunya Rallycross	5.099 km 25.378 km 1.133 km	Tarmac Tarmac + Concrete Dirt + Tarmac

Table 3: The set of inputs that each algorithm receives.

Method	Inputs during Training	Inputs at Test Time
Only Obs	obs	obs
History Input	obs, history	obs, history
RMA	obs, history, context	obs, history
SPARC	obs, history, context	obs, history
Oracle	obs, context	obs, context

- (1) Car Models: we sort all ~500 vehicles by their anomaly score through an isolation forest on the car's contextual features such as mass, length, width, weight distribution, power source type, drive train type, wheel radius, etc. We hold out the 20% most *outlier* vehicles as a test set (OOD) and train on the 80% most *inlier* cars (IND).
- (2) *Power & Mass:* for a more controlled experiment, we pick a relatively standard racing car, but tune its engine power and mass in each training episode to randomly sampled values within the range [75%, 125%] of their defaults. During evaluation, we test on fixed-spaced intervals within [50%, 150%], covering IND and OOD contextual settings.

For the wind-perturbed MuJoCo environments, we similarly train on a certain range of wind speeds, while testing on intervals twice as large. In Gran Turismo, we experiment on three different tracks, presented in Table 2. These tracks represent highly varying settings, with *Catalunya Rallycross* even including a mixed dirt and tarmac racing path.

5.2 Training Details

We repeat our runs with independent random seeds to ensure statistical robustness: three seeds for the compute-heavy Gran Turismo simulator, and five for MuJoCo environments. Key training hyperparameters—such as the history length H, learning rates, and network architectures—are tuned through preliminary experiments with grid search. We train all methods asynchronously, collecting experience on distributed rollout workers. Further training details and analyses are provided in the supplementary material.

5.3 Evaluation Protocol

We evaluate policy performance under two settings:

- **In-Distribution (IND):** Environments with contextual parameters that lie within the training distribution.
- Out-of-Distribution (OOD): Contextual parameters that deviate significantly from the training set, testing the model's generalization capabilities.

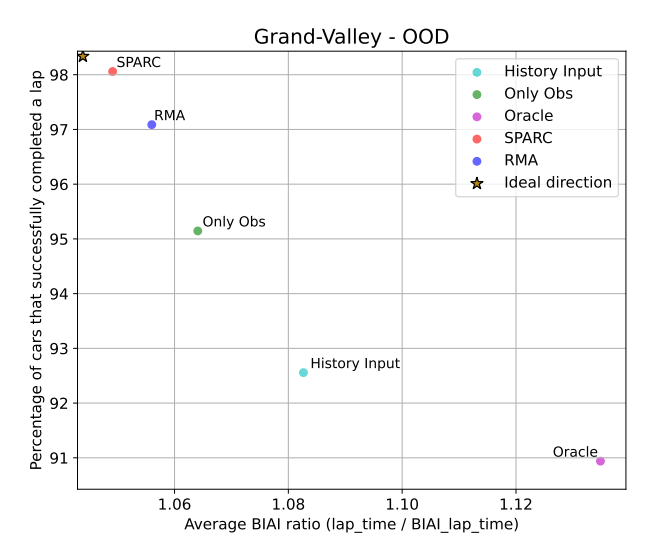


Figure 2: Results on Grand Valley averaged over three seeds. For each algorithm, we plot the percentage of cars that successfully completed laps, and the built-in AI ratio lap time. SPARC is able to complete the most and the fastest laps on out-of-distribution cars.

During training, we regularly evaluate the policy on three predetermined IND settings. These training evaluations form a Pareto-front, from which we select the best model checkpoint for each run. We then test the policy on a wide range of IND & OOD contexts. For *Car Models*, this means all unique vehicles, while for *Power & Mass* and *MuJoCo* we divide the widest context ranges into fixed intervals, providing up to $21^2 = 441$ test environments.

Performance metrics include the return for *MuJoCo* and lap times in *Gran Turismo*. However, for particularly difficult outlier cars, some algorithms may not be able to complete any laps. For this reason, we present the racing results along two dimensions: (1) percentage of cars with a completed lap, and (2) the average lap time. Note that (2) is a biased metric, so (1) needs to be taken into account.

When averaging raw lap times, slower cars have a larger impact on the average. To avoid skewed results, we divide by the built-in AI (BIAI) lap time for each specific car. The BIAI is a classical control method implemented in Gran Turismo 7 to follow a preset driving line. This *BIAI ratio* of RL lap time over BIAI lap time provides an informative normalized value. When a car was unable to complete a lap, we set its BIAI ratio to 2.0 before averaging over all vehicles.

5.4 Baselines

We compare the performance of the following algorithms.

- Only Obs: This QR-SAC (Wurman et al. 2022) policy is trained without any context information. Only the current observation is provided as input.
- **History Input:** A baseline policy (Lee et al. 2020a) that additionally receives a history of observation-action pairs $h_t = (o_{t-H:t-1}, a_{t-H:t-1})$.

Table 4: Performance summary of the *Power & Mass* experiments, averaged over 3 seeds. Results show the mean built-in-AI lap-time ratio (2.0 if no lap completed) across all OOD power & mass settings, and the percentage of these settings with a successfully completed lap (\pm s.e.m.). SPARC completes the most and has the fastest laps.

Method	Built-in-AI lap-time ratio (↓)	Success % (†)
Only Obs	1.0131 ± 0.0136	98.75 ± 1.25
History Input	1.0135 ± 0.0013	98.33 ± 0.10
RMA	1.0004 ± 0.0030	99.17 ± 0.28
SPARC	$\textbf{0.9907} \pm \textbf{0.0011}$	$\textbf{99.90} \pm \textbf{0.10}$
Oracle	0.9962 ± 0.0067	99.27 ± 0.58

- RMA: The two-phase approach of Rapid Motor Adaptation (Kumar et al. 2021), first trains an expert policy with context input, then learns the adapter policy from history.
- **SPARC:** Our single-phase adaptation technique introduced in this work. At test time it only receives an observation-action history and the current observation.
- Oracle: A policy that has access to the ground-truth unencoded contextual features, even at test time.

Benchmarking SPARC against the listed baselines allows us to isolate the benefits of our single-phase training paradigm, especially regarding implementation simplicity and OOD generalization. See Table 3 for a concise overview of the inputs per algorithm.

6 Results

We present the performance of SPARC and several baselines on *Gran Turismo* and *MuJoCo* environments, focusing on generalization to unseen contexts.

6.1 Gran Turismo: Car Models

The scatterplot in Figure 2 summarizes the performance of each algorithm averaged over all out-of-distribution cars on the race track Grand Valley. The results indicate that SPARC outperforms the baselines across unseen vehicles during training. SPARC completes laps with the most cars and with the fastest average built-in AI ratio lap time.

Table 1 provides a quantitative summary of our findings across all three tracks. On IND settings, SPARC is competitive, but it is particularly designed to handle OOD dynamics. When racing untrained cars, SPARC is the fastest of all algorithms without access to context at test time on 2 out of 3 tracks. Furthermore, our method manages to complete laps with the most OOD vehicles on aggregate.

SPARC even outperforms its two-phase counterpart RMA. We believe this occurs because SPARC avoids the brittle selection of a phase-1 checkpoint, required by RMA. Training an adapter ϕ against one checkpoint of ψ can overfit to parts of the context space, while SPARC learns against multiple strong checkpoints over time.

6.2 Gran Turismo: Power & Mass

In Figure 4 we show the difference between (a) the strongest baseline and (b) our method. SPARC is able to complete laps

Table 5: Performance across MuJoCo environments, averaged over 5 seeds. Results show the mean return over all out-of-distribution wind perturbations (\pm s.e.m.). SPARC outperforms all baselines in 2 out of 3 environments.

Method	HalfCheetah-v5 (↑)	Hopper-v5 (↑)	Walker2d-v5 (↑)
Only Obs History Input RMA	5724.51 ± 1624.98 8760.12 ± 161.53 9033.87 ± 634.11	1274.13 ± 133.78 1367.09 ± 67.79 1307.96 ± 45.65	2495.77 ± 220.69 1534.86 ± 144.26 2306.23 ± 222.09
SPARC Oracle	9033.87 ± 034.11 10017.90 ± 476.19 7821.42 ± 1156.77	1348.22 ± 53.67 1710.14 ± 98.98	2500.23 ± 222.09 2528.25 ± 263.58 2325.30 ± 576.48

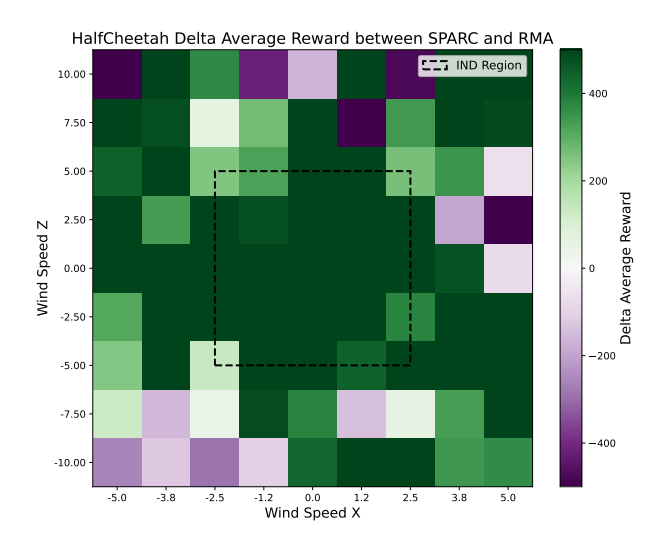


Figure 3: Difference in average return of SPARC versus RMA with varying wind perturbations over 5 seeds. In green: SPARC is better in that wind setting, while in purple: RMA scores higher. Our method outperforms the two-phase baseline across many IND and OOD contextual settings.

in almost all OOD contextual settings, while RMA struggles in the most difficult scenarios of lightweight cars with high engine power. Table 4 provides a summary of the average results across all OOD contexts, indicating that SPARC outperforms all baselines, including the Oracle method. The Oracle does not receive history as part of its inputs, as opposed to other baselines. We believe that SPARC is even able to outperform the Oracle in this environment because knowledge of some history may be useful to mitigate the partial observability in our contextual MDP $\mathcal M$ (Section 3.1). SPARC is the most robust in this experiment—completing laps in all but one setting—and also achieves the fastest average built-in-AI lap-time ratio.

6.3 MuJoCo: Wind Perturbations

In Figure 3, we present results on HalfCheetah by calculating the difference in performance between SPARC and its main baseline RMA, in each wind perturbation tested. The green squares show SPARC outperforming RMA, while purple indicates the opposite. Overall, SPARC beats RMA in significantly more IND and OOD settings, demonstrating a robust performance across varying contexts.

Table 5 shows the OOD results for all baselines and Mu-

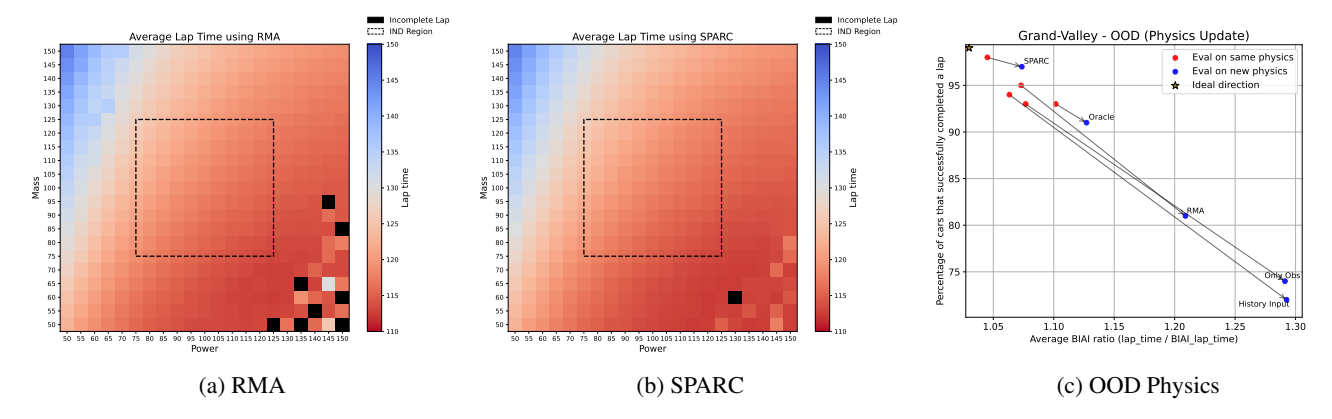


Figure 4: (a) and (b): Lap times on the *Power & Mass* experiment. Colours denote average lap time over 3 seeds (red = fast, blue = slow); black squares indicate at least one unfinished lap. Even though both algorithms are trained only on settings within the IND region (dashed box), SPARC is able to handle challenging OOD settings in the bottom-right corner (high power and low mass). (c): Performance difference between old and new game dynamics. These algorithms have only been trained on old physics settings, and are tested zero-shot on the new physics after a game update of Gran Turismo. SPARC shows the best OOD generalization, with only slightly slower lap times on new dynamics, while other methods degrade significantly.

JoCo environments. Again, SPARC presents strong generalization ability to unseen contexts. On Hopper, the Oracle performs best; note that this baseline has access to true context at test-time, in contrast to all others (see Table 3).

6.4 Transferability to Updated Game Dynamics

The *Gran Turismo* developers regularly deploy game updates, where the simulation physics can be adjusted. Reinforcement learning agents that are trained on previous game dynamics may struggle to adapt. In this section we evaluate policies on the newest game dynamics, while they were solely trained on a previous version of Gran Turismo.

In Figure 4c, we show that SPARC outperforms all baselines in OOD generalization, this time not only across different car models, but also across other unseen environment dynamics. The Oracle policy with access to ground-truth context is not able to finish laps with around 10% of the OOD cars, while SPARC reduces this to less than 5%, with significantly faster lap times. Note that the context $c \in \mathcal{C}$ that we provide to the Oracle contains information about the car model only, as the exact simulator physics adjustments are unknown to us. This missing information highlights the importance of SPARC's ability to adapt to unseen contexts without access to comprehensive contextual details, e.g., when training in simulation and transferring to a real-world environment.

7 Conclusion

This paper introduces SPARC, a novel single-phase adaptation method for robust control in contextual environments. The algorithm unifies context encoding and history-based adaptation into one streamlined training procedure. By eliminating the need for separate phases, SPARC not only simplifies implementation but also facilitates continual learning and deployment in real-world scenarios.

Our extensive experiments in both the high-fidelity Gran

Turismo 7 simulator and various MuJoCo tasks demonstrate that SPARC achieves competitive or superior performance in both in-distribution and OOD settings. In particular, SPARC excels at generalizing to unseen contexts while maintaining robust control, a critical capability for robotics applications where explicit contexts are unknown during deployment.

While our results are promising, the work also highlights opportunities for future research. In particular, testing SPARC on physical robotic platforms and further optimizing its training efficiency remain important next steps. Overall, SPARC represents a significant advance toward practical, adaptable agents that can thrive in dynamic environments.

Acknowledgments

We are grateful to Florian Fuchs for initiating this research project. Further appreciation to everyone at Sony AI—especially the *Gran Turismo* team members—for many fruitful discussions. Finally, we thank all anonymous reviewers who helped to improve the quality of our work.

Ethics Statement

This work advances core machine learning capabilities by improving the performance and generalizability of reinforcement learning agents. While we focus on algorithmic improvements, we acknowledge that, like most technical advances in ML, this work may have various societal impacts. We encourage thoughtful consideration of these implications when building upon this research.

References

Abbasi-Yadkori, Y.; and Neu, G. 2014. Online learning in MDPs with side information. *arXiv preprint* arXiv:1406.6812. (Cited on page 3)

Beck, J.; Jackson, M. T.; Vuorio, R.; and Whiteson, S. 2023. Hypernetworks in Meta-Reinforcement Learning. In *Con-*

- ference on Robot Learning, 1478–1487. PMLR. (Cited on page 3)
- Benjamins, C.; Eimer, T.; Schubert, F.; Biedenkapp, A.; Rosenhahn, B.; Hutter, F.; and Lindauer, M. 2021. CARL: A Benchmark for Contextual and Adaptive Reinforcement Learning. *Eco. Theory RL, NeurIPS.* (Cited on page 1, 2)
- Beukman, M.; Jarvis, D.; Klein, R.; James, S.; and Rosman, B. 2023. Dynamics Generalisation in Reinforcement Learning via Adaptive Context-Aware Policies. *Neural Information Processing Systems*. (Cited on page 2, 3)
- Chen, B.; Liu, Z.; Zhu, J.; Xu, M.; Ding, W.; Li, L.; and Zhao, D. 2021. Context-Aware Safe Reinforcement Learning for Non-Stationary Environments. In *Int. Conf. on Robotics and Automation*. IEEE. (Cited on page 2)
- Cobbe, K.; Hesse, C.; Hilton, J.; and Schulman, J. 2020. Leveraging Procedural Generation to Benchmark Reinforcement Learning. In *Int. Conf. on Machine Learning*. (Cited on page 2)
- Degrave, J.; Felici, F.; Buchli, J.; Neunert, M.; Tracey, B.; Carpanese, F.; Ewalds, T.; Hafner, R.; Abdolmaleki, A.; de las Casas, D.; et al. 2022. Magnetic control of tokamak plasmas through deep reinforcement learning. *Nature*, 602(7897): 414–419. (Cited on page 1)
- Duan, Y.; Schulman, J.; Chen, X.; Bartlett, P. L.; Sutskever, I.; and Abbeel, P. 2016. RL²: Fast Reinforcement Learning via Slow Reinforcement Learning. *arXiv preprint arXiv:1611.02779*. (Cited on page 3)
- Finn, C.; Abbeel, P.; and Levine, S. 2017. Model-Agnostic Meta-Learning for Fast Adaptation of Deep Networks. In *International Conference on Machine Learning*, 1126–1135. PMLR. (Cited on page 3)
- Gisslén, L.; Eakins, A.; Gordillo, C.; Bergdahl, J.; and Tollmar, K. 2021. Adversarial Reinforcement Learning for Procedural Content Generation. In 2021 IEEE Conference on Games (CoG). IEEE. (Cited on page 2)
- Grooten, B.; Tomilin, T.; Vasan, G.; Taylor, M. E.; Mahmood, A. R.; Fang, M.; Pechenizkiy, M.; and Mocanu, D. C. 2024. MaDi: Learning to Mask Distractions for Generalization in Visual Deep Reinforcement Learning. *Autonomous Agents and Multiagent Systems*. (Cited on page 3)
- Haarnoja, T.; Zhou, A.; Abbeel, P.; and Levine, S. 2018. Soft Actor-Critic: Off-Policy Maximum Entropy Deep Reinforcement Learning with a Stochastic Actor. In *International Conference on Machine Learning*, 1861–1870. PMLR. (Cited on page 10)
- Hallak, A.; Di Castro, D.; and Mannor, S. 2015. Contextual Markov Decision Processes. *arXiv preprint arXiv:1502.02259*. (Cited on page 3)
- Hansen, N.; Su, H.; and Wang, X. 2021. Stabilizing Deep Q-Learning with ConvNets and Vision Transformers under Data Augmentation. *Neural Information Processing Systems*, 34: 3680–3693. (Cited on page 2)
- Huang, Y.; Peng, P.; Zhao, Y.; Chen, G.; and Tian, Y. 2022. Spectrum Random Masking for Generalization in Image-based Reinforcement Learning. *Neural Information Processing Systems*, 35. (Cited on page 3)

- Kingma, D. P.; and Ba, J. 2015. Adam: A Method for Stochastic Optimization. *International Conference for Learning Representations*. (Cited on page 10)
- Kirk, R.; Zhang, A.; Grefenstette, E.; and Rocktäschel, T. 2023. A Survey of Zero-shot Generalisation in Deep Reinforcement Learning. *Journal of Artificial Intelligence Research*, 76: 201–264. (Cited on page 1, 3)
- Kumar, A.; Fu, Z.; Pathak, D.; and Malik, J. 2021. RMA: Rapid Motor Adaptation for Legged Robots. *Robotics: Science and Systems*. (Cited on page 1, 2, 3, 6, 22)
- Lahmer, S.; Mason, F.; Chiariotti, F.; and Zanella, A. 2024. Fast Context Adaptation in Cost-Aware Continual Learning. *IEEE Transactions on Machine Learning in Communications and Networking*. (Cited on page 2)
- Langford, J. 2017. Contextual Reinforcement Learning. In 2017 IEEE International Conference on Big Data, 3–3. (Cited on page 2)
- Laskin, M.; Lee, K.; Stooke, A.; Pinto, L.; Abbeel, P.; and Srinivas, A. 2020. Reinforcement learning with augmented data. *Advances in neural information processing systems*, 33: 19884–19895. (Cited on page 2)
- Lee, J.; Hwangbo, J.; Wellhausen, L.; Koltun, V.; and Hutter, M. 2020a. Learning quadrupedal locomotion over challenging terrain. *Science Robotics*, 5(47). (Cited on page 2, 3, 5)
- Lee, K.; Seo, Y.; Lee, S.; Lee, H.; and Shin, J. 2020b. Context-aware Dynamics Model for Generalization in Model-Based Reinforcement Learning. In *International Conference on Machine Learning*. (Cited on page 2)
- Leon, B. G.; Riccio, F.; Subramanian, K.; Wurman, P. R.; and Stone, P. 2024. Discovering Creative Behaviors through DUPLEX: Diverse Universal Features for Policy Exploration. In *Neural Information Processing Systems*. (Cited on page 2)
- Lyle, C.; Rowland, M.; Dabney, W.; Kwiatkowska, M.; and Gal, Y. 2022. Learning Dynamics and Generalization in Reinforcement Learning. *Int. Conf. on Machine Learning*. (Cited on page 2)
- Mahmood, A. R.; Korenkevych, D.; Vasan, G.; Ma, W.; and Bergstra, J. 2018. Benchmarking Reinforcement Learning Algorithms on Real-World Robots. In *Conf. on Robot Learning*, 561–591. PMLR. (Cited on page 1)
- Morrill, D.; Walsh, T. J.; Hernandez, D.; Wurman, P. R.; and Stone, P. 2023. Composing Efficient, Robust Tests for Policy Selection. In *Uncertainty in Artificial Intelligence*, 1456–1466. PMLR. (Cited on page 3)
- Peng, X. B.; Andrychowicz, M.; Zaremba, W.; and Abbeel, P. 2018. Sim-to-Real Transfer of Robotic Control with Dynamics Randomization. In *Int. Conf. on Robotics and Automation (ICRA)*. IEEE. (Cited on page 2)
- Prasanna, S.; Farid, K.; Rajan, R.; and Biedenkapp, A. 2024. Dreaming of Many Worlds: Learning Contextual World Models Aids Zero-Shot Generalization. *Reinforcement Learning Conference*. (Cited on page 2)

- Rabinowitz, N.; Perbet, F.; Song, F.; Zhang, C.; Eslami, S. A.; and Botvinick, M. 2018. Machine Theory of Mind. In *International Conference on Machine Learning*, 4218–4227. PMLR. (Cited on page 3)
- Rezaei-Shoshtari, S.; Morissette, C.; Hogan, F. R.; Dudek, G.; and Meger, D. 2023. Hypernetworks for Zero-shot Transfer in Reinforcement Learning. In *The AAAI Conference on Artificial Intelligence*. (Cited on page 3)
- Schulman, J.; Wolski, F.; Dhariwal, P.; Radford, A.; and Klimov, O. 2017. Proximal Policy Optimization Algorithms. *arXiv preprint arXiv:1707.06347*. (Cited on page 3)
- Tobin, J.; Fong, R.; Ray, A.; Schneider, J.; Zaremba, W.; and Abbeel, P. 2017. Domain Randomization for Transferring Deep Neural Networks from Simulation to the Real World. In *International Conference on Intelligent Robots and Systems (IROS)*, 23–30. IEEE. (Cited on page 2)
- Todorov, E.; Erez, T.; and Tassa, Y. 2012. MuJoCo: A physics engine for model-based control. In 2012 IEEE/RSJ International Conference on Intelligent Robots and Systems, 5026–5033. IEEE. (Cited on page 4)

- Wang, J. X.; Kurth-Nelson, Z.; Tirumala, D.; Soyer, H.; Leibo, J. Z.; Munos, R.; Blundell, C.; Kumaran, D.; and Botvinick, M. 2016. Learning to reinforcement learn. *arXiv* preprint arXiv:1611.05763. (Cited on page 3)
- Wang, S.; Wu, Z.; Hu, X.; Wang, J.; Lin, Y.; and Lv, K. 2024. What Effects the Generalization in Visual Reinforcement Learning: Policy Consistency with Truncated Return Prediction. *Proceedings of the AAAI Conference on Artificial Intelligence*, 38(6): 5590–5598. (Cited on page 2)
- Wurman, P. R.; Barrett, S.; Kawamoto, K.; MacGlashan, J.; Subramanian, K.; Walsh, T. J.; Capobianco, R.; Devlic, A.; Eckert, F.; Fuchs, F.; et al. 2022. Outracing champion Gran Turismo drivers with deep reinforcement learning. *Nature*, 602(7896): 223–228. (Cited on page 1, 3, 4, 5, 10, 12)
- Yu, W.; Tan, J.; Liu, C. K.; and Turk, G. 2017. Preparing for the Unknown: Learning a Universal Policy with Online System Identification. *Robotics: Science and Systems*. (Cited on page 2)

Appendix

A Training and Implementation Details

All experiments are conducted using the off-policy QR-SAC algorithm (Wurman et al. 2022) as the base reinforcement learning method. In the MuJoCo experiments, we train for 3M policy updates. For Gran Turismo, in the Power & Mass setting we perform 6M updates, while across Car Models we train for 9M steps. The famously long and difficult N"urburgring track is an exception, where we perform additional updates: 12M, see Table 6.

We tune the history length (see Section B.2) and the history adapter's learning rate (values: $\{2.5 \times 10^{-4}, 2.5 \times 10^{-5}\}$). The list of hyperparameters used for training our Gran Turismo and MuJoCo experiments is presented in Table 7.

In each training episode, a new IND setting is sampled according to Equation 1, determining either the wind speeds, the car's power & mass, or the full car model. Generalization complexity is further raised for the *Car Model* experiment by sampling uniformly over 9 tire types, from least traction *Comfort Hard* up to most traction *Racing Soft*.

A.1 Code

The code for *Gran Turismo* 7 is proprietary. The game runs exclusively on PlayStation (PS4 and PS5), which we use for training. However, for reproducibility we do provide open-source code for the multiple wind-perturbed MuJoCo environments that we designed, in the supplementary material. Furthermore, see Algorithm 1 for pseudocode of our algorithm SPARC. The resulting adapter policy $\pi_{\theta}^{ad}(o,h)$ no longer requires the context c as input, and is the model deployed at test time.

Environment	Training steps
MuJoCo	3M
Gran Turismo (Power & Mass)	6M
Gran Turismo (Car Models)	9M (Nürburgring track: $12M$)

Table 6: Number of training steps for each environment.

A.2 Model Architecture

The architecture of SPARC used in our experiments is detailed in Table 8. We use QR-SAC as the base reinforcement learning algorithm for the expert policy, which involves two critic networks and two critic target networks. All four of these have the same architecture, with access to the true context c. This is possible since the critics are not needed at deployment, only during training. We use 32 quantiles within the critic networks of QR-SAC.

The observation o is a large vector of relevant information, similar to the one used by Wurman et al. (2022). The action a has a dimension of 2 for Gran Turismo, and varying numbers for the MuJoCo environments. For our MuJoCo experiments, we decrease the width of the FC layers from 2048 and 64 to 256 and 32, respectively.

Hyperparameter	Gran Turismo	MuJoCo
Optimizer	Adam (Kingma and Ba 2015)	Adam
Batch size (B)	1024	32
History length (H)	50	50
History adapter learning rate (α_{ad})	2.5×10^{-4}	3×10^{-4}
SAC learning rate for π^{ex} and critics (α_{SAC})	2.5×10^{-5}	3×10^{-4}
Target critics update rate (τ)	0.005	0.005
Global norm of critics gradient clipping	10	10
Discount factor (γ)	0.9896	0.99
SAC entropy temperature (Haarnoja et al. 2018)	0.01	0.01
Number of quantiles	32	32

Table 7: Training hyperparameters for Gran Turismo and MuJoCo experiments.

Table 8: Model architecture of SPARC. See Figure 1 for a schematic overview.

Layer Description	Input Dimensions	Output Dimensions
Expert Policy π^{ex}		
Observation Encoder		
FC: 2048 units, ReLU	o	2048
FC: 2048 units, ReLU	2048	2048
Context Encoder		
FC: 64 units, ReLU	c	64
FC: 64 units, ReLU	64	64
Decision Layers		
FC: 2048 units, ReLU	2112 (2048 + 64)	2048
FC: 2048 units, ReLU	2048	2048
FC: 2a units, Tanh	2048	2a
Adapter Policy π^{ad}		
Observation Encoder		
FC: 2048 units, ReLU	0	2048
FC: 2048 units, ReLU	2048	2048
History Adapter		
FC: 64 units, ReLU	(o + a)x50	64x50
Conv1D: 32 filters, kernel 8, stride 4, ReLU	64x50	32x13
Conv1D: 32 filters, kernel 5, stride 1, ReLU	32x13	32x13
Conv1D: 32 filters, kernel 5, stride 1, ReLU	32x13	32x13
Flatten	32x13	416
FC: 64 units, ReLU	416	64
Decision Layers		
FC: 2048 units, ReLU	2112 (2048 + 64)	2048
FC: 2048 units, ReLU	2048	2048
FC: 2a units, Tanh	2048	2a
Critic Networks		
Observation + Action Encoder		
FC: 2048 units, ReLU	o + a	2048
FC: 2048 units, ReLU	2048	2048
Context Encoder		
FC: 64 units, ReLU	c	64
FC: 64 units, ReLU	64	64
Decision Layers		
FC: 2048 units, ReLU	2112 (2048 + 64)	2048
FC: 2048 units, ReLU	2048	2048
FC: 32 units, identity	2048	32

Algorithm 1: SPARC: Single-Phase Adaptation for Robust Control **Input**: Environment \mathcal{M} with latent context c (observable only during training) History length H, replay buffer \mathcal{D} , batch size BDiscount γ , target-update rate τ , learning rates α_{SAC} , α_{ad} **Output:** Adapter policy $\pi_{\scriptscriptstyle A}^{ad}$ 1 Initialise: 2 Expert policy π^{ex} with context encoder ψ Adapter policy π^{ad} with history adapter ϕ Critic networks Q^{ex} and target critics $\tilde{Q}^{ex} \leftarrow Q^{ex}$ History $h \leftarrow \mathbf{0}^H$ Sample IND context c for environment \mathcal{M} 7 for t = 1, 2, ... do // Collect experience with adapter policy 8 Observe o_t from environment \mathcal{M}_c Sample action $a_t \sim \pi_{\theta}^{ad}(o_t, h_t)$ 9 Concatenate (o_t, a_t) to history $h_t = (o_{t-H:t-1}, a_{t-H:t-1})$; (and pop last entry) 10 Execute a_t , receive reward r_t , next observation o_{t+1} and done flag d_t 11 Store transition $(o_t, a_t, r_t, o_{t+1}, d_t, h_t, c) \rightarrow \mathcal{D}$ 12 if $|\mathcal{D}| > B$ then 13 Sample minibatch \mathcal{B} of B tuples from \mathcal{D} 14 // Expert Policy update via QR-SAC $\theta^Q \leftarrow \theta^Q - \alpha_{SAC} \nabla_{\theta^Q} \mathcal{L}_{SAC}(\pi^{ex}, Q^{ex}, \tilde{Q}^{ex})$ 15 $\theta^{ex} \leftarrow \theta^{ex} + \alpha_{SAC} \nabla_{\theta^{ex}} J_{SAC}(\pi^{ex})$ 16 // History Adapter regression $\theta^{\phi} \leftarrow \theta^{\phi} - \alpha_{ad} \nabla_{\theta^{\phi}} \| \phi(h) - \psi(c) \|_{2}^{2}$ 17 // Polyak averaging of target critics $\tilde{Q}^{ex} \leftarrow (1-\tau)\tilde{Q}^{ex} + \tau Q^{ex}$ 18 // Copy obs. encoder & decision layers from π^{ex} to π^{ad} $\theta^{ad} \leftarrow \text{copy_modules}(\theta^{ex}, \theta^{ad})$ 19

A.3 Rollouts and Distributed Training

reset history $h \leftarrow \mathbf{0}^H$

reset environment \mathcal{M} ; sample new IND context c

if d_t then

20

21

22

We train our algorithms asynchronously, performing rollouts on up to 20 distributed PlayStations simultaneously for Gran Turismo runs. The collected experience is added to a central replay buffer, from which a single GPU trains the neural networks. We use NVIDIA A100 GPUs with 40GB of memory. The wall-clock training time of an average Gran Turismo run is about 6 days, for MuJoCo it is approximately 14 hours. See Wurman et al. (2022) for further details on the Gran Turismo training setup.

At the start of each episode, we sample a contextual setting uniformly at random from the in-distribution (IND) set. For Gran Turismo, the agent's initial position is randomly chosen from on-track regions as well as from off-track zones to the left and right, extending up to 5% of the track width. The agent is oriented to face a point 30 meters ahead along the center line, and its initial speed is drawn uniformly from 0 to 104.607 km/h. Each episode runs for up to 150 seconds before being reset.



(a) IND cars sampled from the \sim 400-vehicle training set. The Mazda, Lamborghini, and Lexus (from left to right) are representative, standard racing cars in *Gran Turismo 7*.



(b) OOD cars drawn from the \sim 100-vehicle test set. The racing kart, the Tomahawk, and the Toyota pickup truck (from left to right) are highly unusual outlier vehicles.

Figure 5: Illustrative in-distribution (IND) versus out-of-distribution (OOD) vehicles used in our *Gran Turismo* 7 experiments.

A.4 Race Cars

As detailed in Section 5, we hold out the 20% most *outlier* vehicles as a test set (OOD) and train on the 80% most *inlier* cars (IND). This means we train on about \sim 400 vehicles, while testing on \sim 100 unseen cars. In Figures 5a and 5b we present a few examples of IND and OOD vehicles, respectively. The sampled cars in these figures are from left to right:

Example In-Distribution cars (Figure 5a)

- Mazda3 '19
- Lamborghini Aventador LP 700-4 '11
- Lexus RC F GT3 '17

Example Out-of-Distribution cars (Figure 5b)

- GT Racing Kart 125 Shifter
- Dodge SRT Tomahawk X Vision GT
- Toyota Tundra TRD Pro '19

The **kart** (on the left in Figure 5b) is one of the most outlier vehicles: very tiny and over-responsive. The **Tomahawk** (in the middle) is extremely fast and also famously difficult to control. The Toyota **pickup truck** (on the right) is an outlier in its mass, being significantly heavier and bulkier than most IND cars.

A.5 Race Tracks

We evaluate our approach on three diverse tracks in Gran Turismo 7: Grand Valley Highway 1, Nürburgring 24h, and Circuit de Barcelona - Catalunya Rallycross. These tracks vary widely in length, layout, and surface composition, enabling robust testing of our model's generalization capabilities.

- Grand Valley is a medium-length road track featuring tight turns, a tunnel section, and a bridge crossing. It provides a balanced mix of technical and high-speed sections.
- Nürburgring is the longest and one of the most complex tracks in the game, combining the Grand Prix circuit with the Nordschleife. Its high difficulty and track length pose a significant generalization challenge.
- Catalunya Rallycross is the shortest of the three. It introduces mixed terrain, with both asphalt and dirt sections. Driving here requires a distinct policy due to the lower traction and rapid transitions between surface types.

The map layouts of these tracks are shown in Figure 6, while in-game screenshots can be found in Figure 7. Exact track lengths and characteristics are summarized in Table 2.

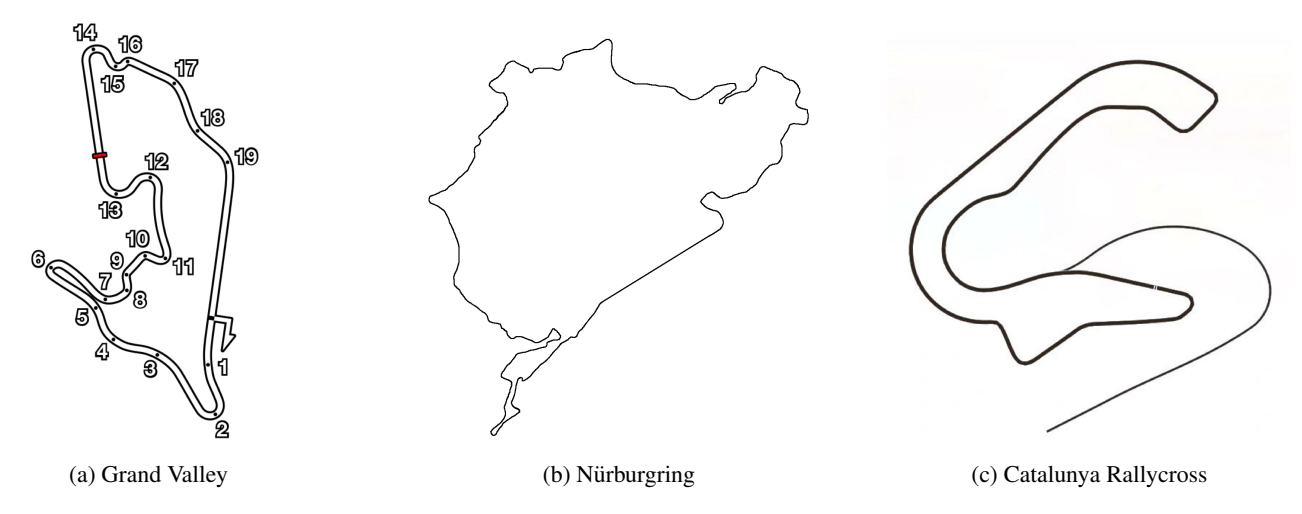


Figure 6: Map layouts of the three tracks in Gran Turismo 7 used in our experiments. Note that these are not in the same scale, Nürburgring is by far the longest track. Catalunya Rallycross is the shortest and features a separate start ramp, which is not a part of our experiments. See Table 2 for the exact lengths of the tracks.



Figure 7: In-game pictures of the three tracks in Gran Turismo 7 used in our experiments. The Grand Valley track is placed on a regular road, going over a bridge and a through a tunnel. Nürburgring is a replica of the real-world race track located in Germany. Catalunya Rallycross is a mixed surface track, with tarmac and dirt areas. Specific dirt tires are required for this track.

B Further Analysis

To gain a deeper understanding of the contributions of our design choices, we perform an analysis of key factors, including the ideal rollout policy (Section B.1) and the optimal history length (Section B.2).

B.1 Selecting the Ideal Rollout Policy

In this ablation, we compare the performance of SPARC under two scenarios: (i) when experience is collected with the expert policy (π^{ex}), or (ii) when this is done by the adapter policy (π^{ad}). As detailed in Section 4.2, by default SPARC performs rollouts with the adapter policy to ensure a more on-policy style of learning for the final product, which is π^{ad} .

Table 9 presents results across all IND and OOD cars on three tracks. Although the differences are small, the results demonstrate that naively using π^{ex} for rollouts leads to slower lap times on 2 out of 3 tracks when looking at OOD generalization. Moreover, SPARC finishes every track with at least as many OOD cars as the alternative method.

B.2 Optimal History Length

We perform a sensitivity analysis of SPARC to different lengths of the observation-action history H. Recall from Figure 1 that SPARC's history adapter ϕ uses this recent experience to recognize its current contextual environment. The history input is defined as $h_t = (o_{t-H:t-1}, a_{t-H:t-1}) \in \mathcal{H}$, where $\mathcal{H} = (\mathcal{O} \times \mathcal{A})^H$ is the space of possible histories.

The results in Figure 8 show that a history length of H=50 timesteps seems to be optimal for SPARC. Too few observation-action pairs do not provide enough information to robustly distinguish between contexts, whereas too many may distract the agent and waste computational resources.

Table 9: Ablation on rollout policy. Results across all IND/OOD cars and 3 seeds. Mean \pm s.e.m. of laptime BIAI ratio and % successful laps. Especially on OOD, naively collecting experience with the expert policy (π^{ex}) generally does not perform as well as directly using the adapter policy (π^{ad}) for rollouts.

Method	IND		OOD	
	BIAI ratio (↓)	Success % (†)	BIAI ratio (↓)	Success % (†)
Grand Valley SPARC (π^{ex} rollouts) SPARC	0.9922 ± 0.0034 0.9999 ± 0.0061	100.0 ± 0.00 99.76 ± 0.14		98.06 ± 0.00 98.06 ± 0.56
$N\ddot{u}rburgring$ SPARC (π^{ex} rollouts) SPARC	$egin{array}{l} \textbf{1.0107} \pm \textbf{0.0150} \\ 1.0254 \pm 0.0061 \end{array}$	96.93 ± 1.21 95.87 ± 0.49	1.1531 ± 0.0158 1.1199 ± 0.0076	85.44 ± 1.12 89.00 ± 0.86
Catalunya Rallycross SPARC (π^{ex} rollouts) SPARC	0.9434 ± 0.0012 0.9432 ± 0.0027	$100.00 \pm 0.00 \\ 100.00 \pm 0.00$	0.9659 ± 0.0032 0.9631 ± 0.0026	$100.00 \pm 0.00 \\ 100.00 \pm 0.00$

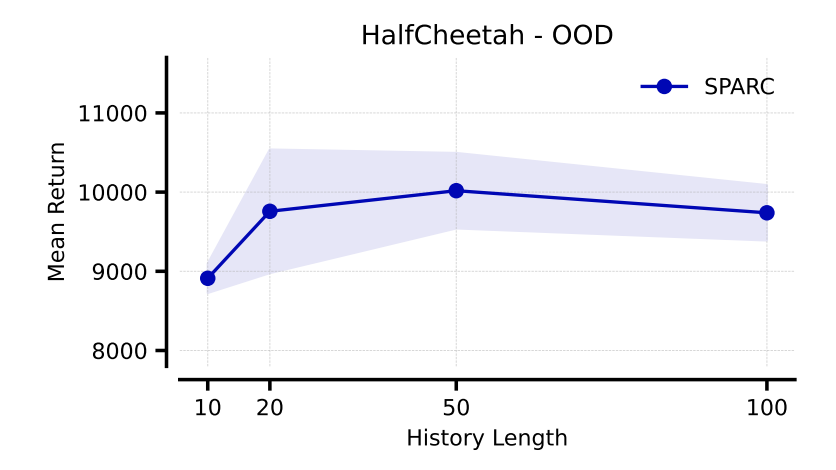


Figure 8: Analysis of the optimal history length for SPARC, averaged over 5 seeds (\pm s.e.m.). We show the mean return over all tested out-of-distribution wind perturbations. A history length of 50 yields the highest average return.

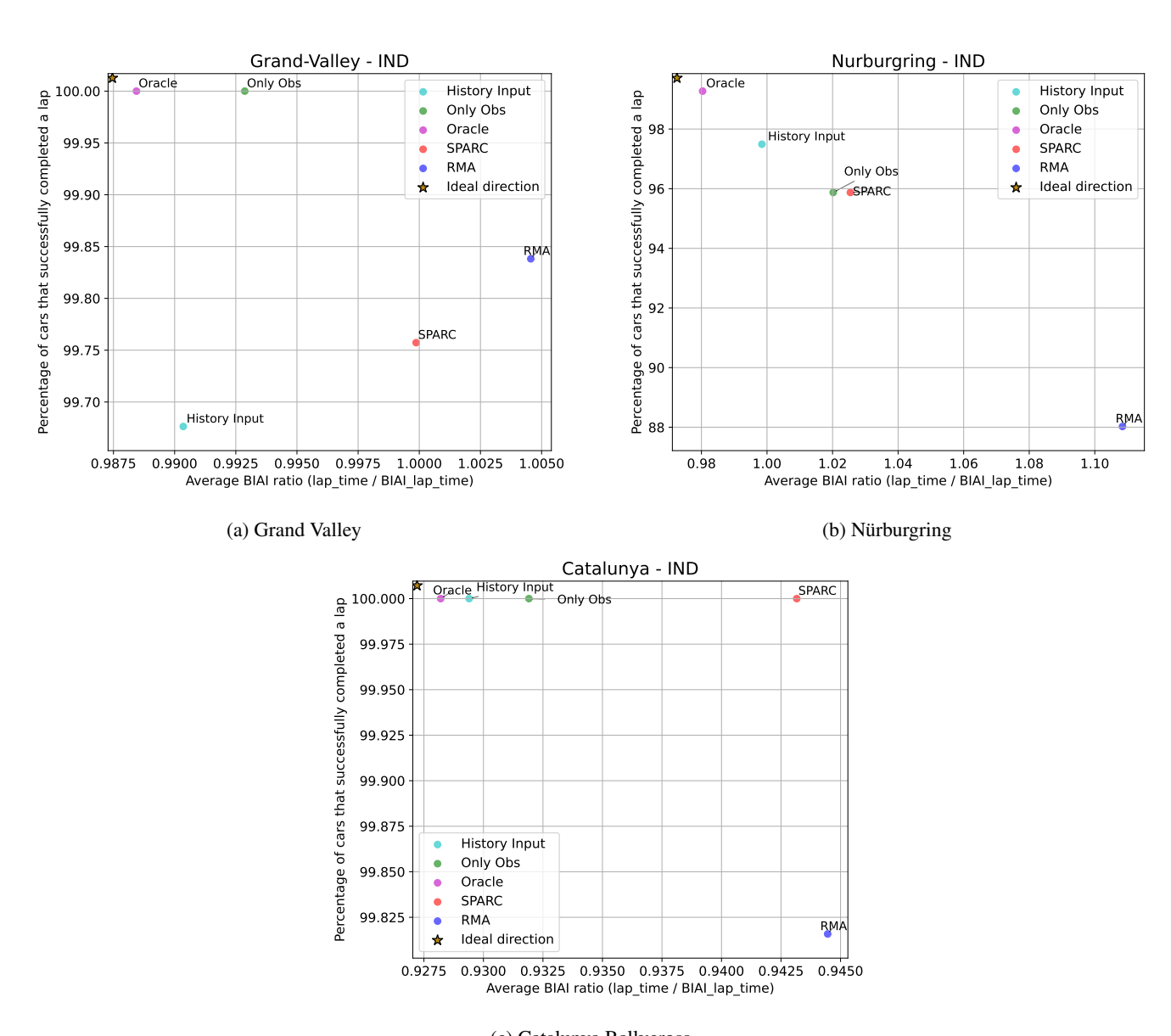
C Additional Results

In this section we provide the graphs and heatmaps of all our experiments. We start with *Gran Turismo*, showing the *Car Models* generalization experiments in Section C.1 and the *Power & Mass* runs in Section C.2. The MuJoCo experiments are presented in Section C.3.

C.1 Gran Turismo: Car Models

Figure 9 (IND) and Figure 10 (OOD) show the full scatter plots of built-in–AI (BIAI) lap–time ratio versus completion rate for every algorithm on each of the three tracks. Each marker corresponds to the average over three independent seeds. These plots make the trade-off between speed and reliability visible at a glance: points closer to the upper–left corner denote faster laps and a higher percentage of completed cars.

Across all tracks, SPARC is on or near the OOD Pareto front, despite lacking privileged context at test time. Note that on the IND plots, the numbers on the axes are generally much closer together than with OOD cars. Table 1 summarises these results numerically. SPARC attains the best out-of-distribution BIAI ratio on two out of three tracks and, averaged over all cars and circuits, completes the most laps with OOD vehicles.



(c) Catalunya Rallycross

Figure 9: Built-in-AI ratio lap times and the percentage of cars that are able to complete a lap for **in-distribution** (**IND**) vehicles. SPARC is designed to generalize well on OOD contexts, but also attains results relatively close to the Oracle baseline in the IND setting. Note that the numbers on these axes contain smaller intervals than the OOD plot (Figure 10).

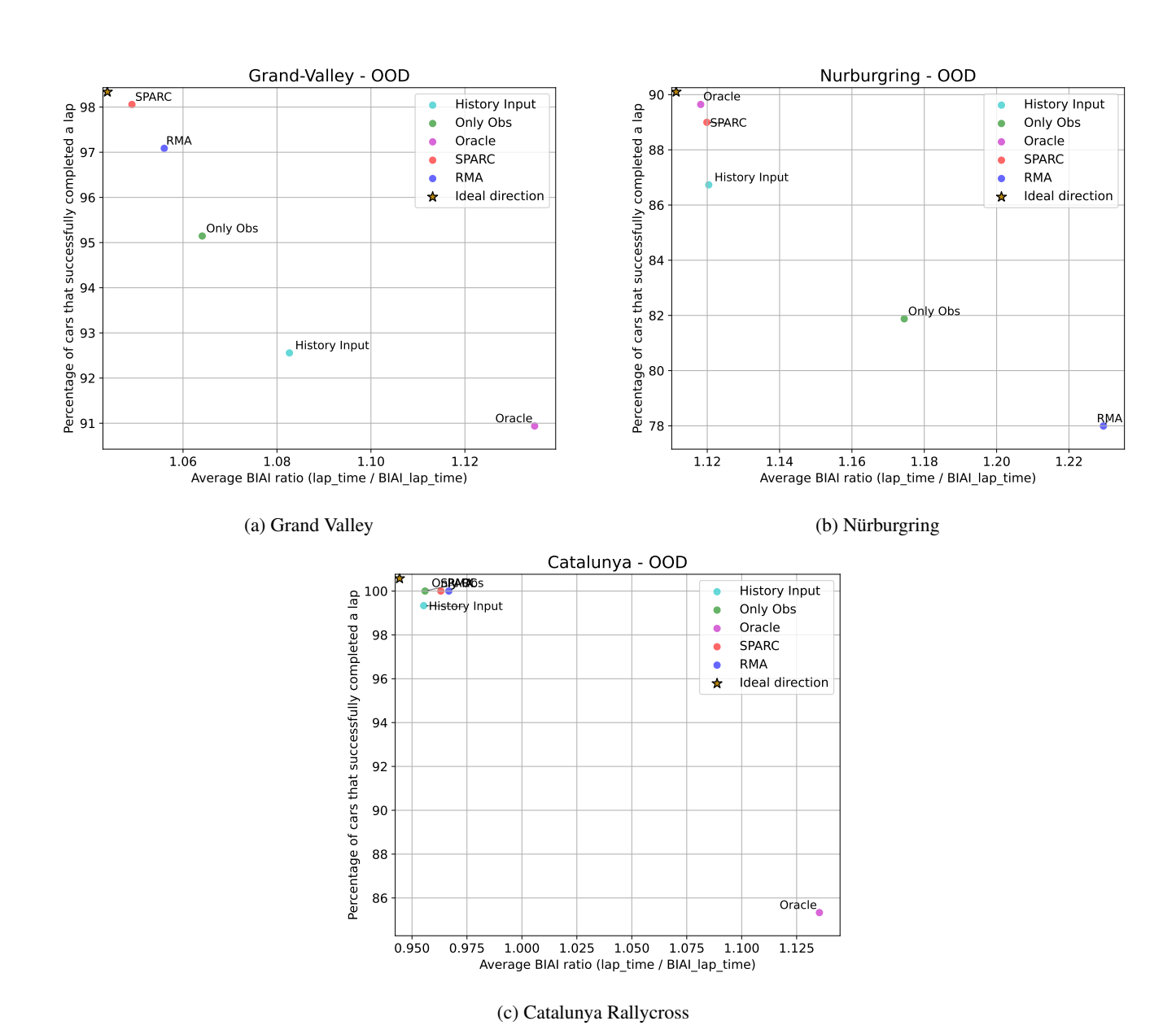


Figure 10: Built-in-AI ratio lap times and the percentage of cars that are able to complete a lap for **out-of-distribution (OOD)** vehicles. On Grand Valley SPARC has the fastest laps and finishes the most OOD cars. On Nürburgring, only the Oracle (which has access to priviledged context at test time) is able to surpass SPARC. The mixed dirt-and-tarmac track (Catalunya Rallycross) is much shorter in length, and thus many algorithms are able to complete laps with all cars.

Table 10: Performance summary on **IND** vehicles for the physics update experiment on Grand Valley. Results show the mean built-in AI (BIAI) ratio across cars. Additionally, we show the percentage of cars with a successfully completed lap. SPARC suffers only a modest slowdown (+0.027) and retains 98% completion, outperforming all non-Oracle baselines.

Method	Before Physics Update		After Physics Update	
	BIAI ratio (↓)	Success (%) (†)	BIAI ratio (↓)	Success (%) (†)
Only Obs	0.9902	100.0	1.1334	89.08
History Input	0.9932	99.27	1.1100	89.32
RMA	1.0093	99.27	1.0584	95.15
SPARC	0.9964	100.0	1.0234	98.30
Oracle	0.9880	100.0	0.9981	99.76

Table 11: Performance summary on **OOD** vehicles for the physics update experiment on Grand Valley. Results show the mean built-in AI (BIAI) ratio across cars. Additionally, we show the percentage of cars with a successfully completed lap. SPARC maintains the highest completion rate (97%) and the fastest lap-times (1.0736) among all methods.

Method	Before Physics Update		After Physics Update	
1v10tillod	BIAI ratio (↓)	Success (%) (†)	BIAI ratio (↓)	Success (%) (†)
Only Obs	1.0769	93.20	1.2912	74.76
History Input	1.0633	94.17	1.2926	72.82
RMA	1.0729	95.15	1.2089	81.55
SPARC	1.0451	98.06	1.0736	97.09
Oracle	1.1016	93.20	1.1271	91.26

Robustness to a physics patch. The March-2025 update to *Gran Turismo* 7 subtly altered the vehicle-dynamics model. To measure zero-shot transfer we evaluate agents trained on the *old* physics on Grand Valley *before* and *after* the patch. Section 6.4 showed a plot with OOD dynamics *and* cars, but in Figure 11 we evaluate on the in-distribution cars seen during training. Although the vehicles themselves are familiar, the simulator's updated physics offer an unseen domain shift, so each agent must generalise zero-shot to new dynamics. As the plot shows, SPARC preserves both speed and reliability under this shift, while the other baselines without access to contextual information suffer noticeable drops in completion rate and/or lap-time. This highlights that SPARC's single-phase adaptation is not merely memorising vehicle-specific behaviour; it learns transferrable representations that remain robust when the underlying environment changes.

Table 10 reports results on in-distribution (IND) cars, while Table 11 repeats the test on out-of-distribution (OOD) cars. Each table lists the mean built-in–AI (BIAI) lap-time ratio (↓ lower is better) and the percentage of cars that complete a lap (↑). Across both IND and OOD car sets, SPARC shows the smallest increase in lap-time ratio and the least drop in completion rate among methods that do *not* receive privileged context at test time, demonstrating strong resilience to unforeseen dynamics changes.

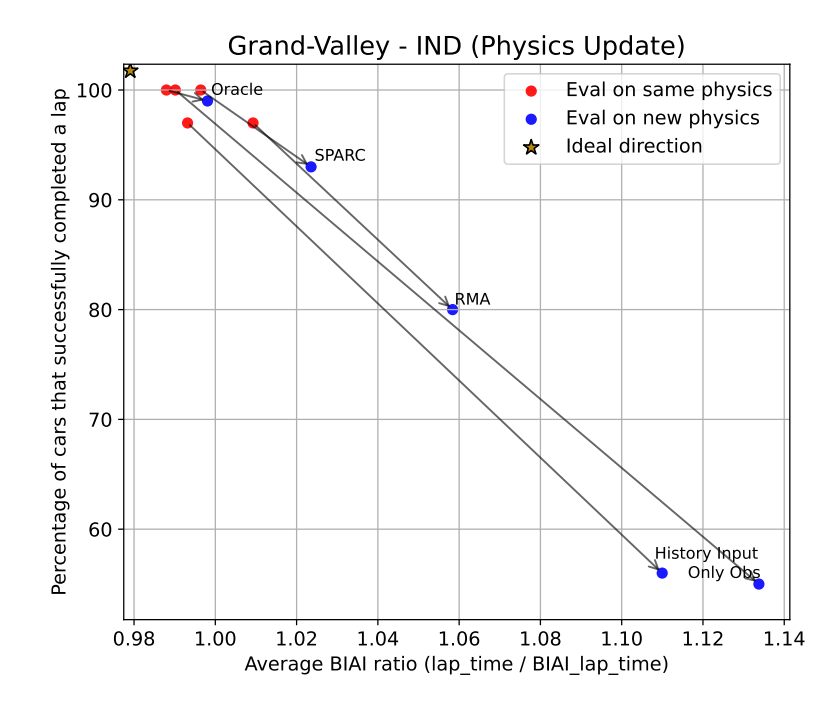


Figure 11: Performance difference between old and new game dynamics. These algorithms have only been trained on old physics, and are tested zero-shot for generalization to the new environment. This graph is on the set of IND cars, but the new physics is out-of-distribution. SPARC and the Oracle baseline have the lowest drops in performance. See Figure 4c for the plot with OOD cars.

C.2 Gran Turismo: Power & Mass

For a controlled stress-test, in Section 6.2 we picked a single baseline car and randomized its *engine power* (x-axis) and *vehicle mass* (y-axis) independently in every episode. In this section, we present additional results from that experiment. The dashed box in the middle of each plot marks the in-distribution training region $[75\%, 125\%] \times [75\%, 125\%]$; everything outside is held-out OOD. Black squares denote settings where at least one evaluation seed failed to finish a lap.

IND results. Table 12 reports averages *inside* the dashed box, as opposed to the OOD results from Table 4. All methods finish virtually every lap, and SPARC matches the two-phase RMA and the privileged Oracle on both speed (BIAI ≈ 0.981) and reliability (100% completion).

OOD results. Figures 12 and 13 visualise performance across the entire $[50\%, 150\%]^2$ grid. Colour encodes either raw lap time (Figure 12) or BIAI ratio (Figure 13); cooler colours indicate slower driving. Outside the training box, Only-Obs, History-Input, and RMA accumulate many black squares in the lower-right corner (the difficult contextual setting of light cars with powerful engines), whereas SPARC only fails in a single extreme cell and achieves visibly faster laps over the viable region. This qualitative picture matches the quantitative OOD numbers in Table 4: SPARC completes 99.9% of OOD settings and records the lowest average BIAI ratio (0.9907).

Table 12: Performance summary of the *Power & Mass* experiments (**IND**), averaged over 3 seeds. Results show the mean built-in-AI lap-time ratios and the percentage of settings with a successfully completed lap (\pm s.e.m.). All methods finish almost every lap; SPARC is tied with RMA and Oracle for fastest average time.

Method	Built-in-AI lap-time ratio (↓)	Success (†)
Only Obs	0.9924 ± 0.0028	99.72 ± 0.28
History Input	0.9868 ± 0.0017	100.00 ± 0.00
RMA	0.9810 ± 0.0002	100.00 ± 0.00
SPARC	0.9810 ± 0.0002	100.00 ± 0.00
Oracle	0.9811 ± 0.0004	100.00 ± 0.00

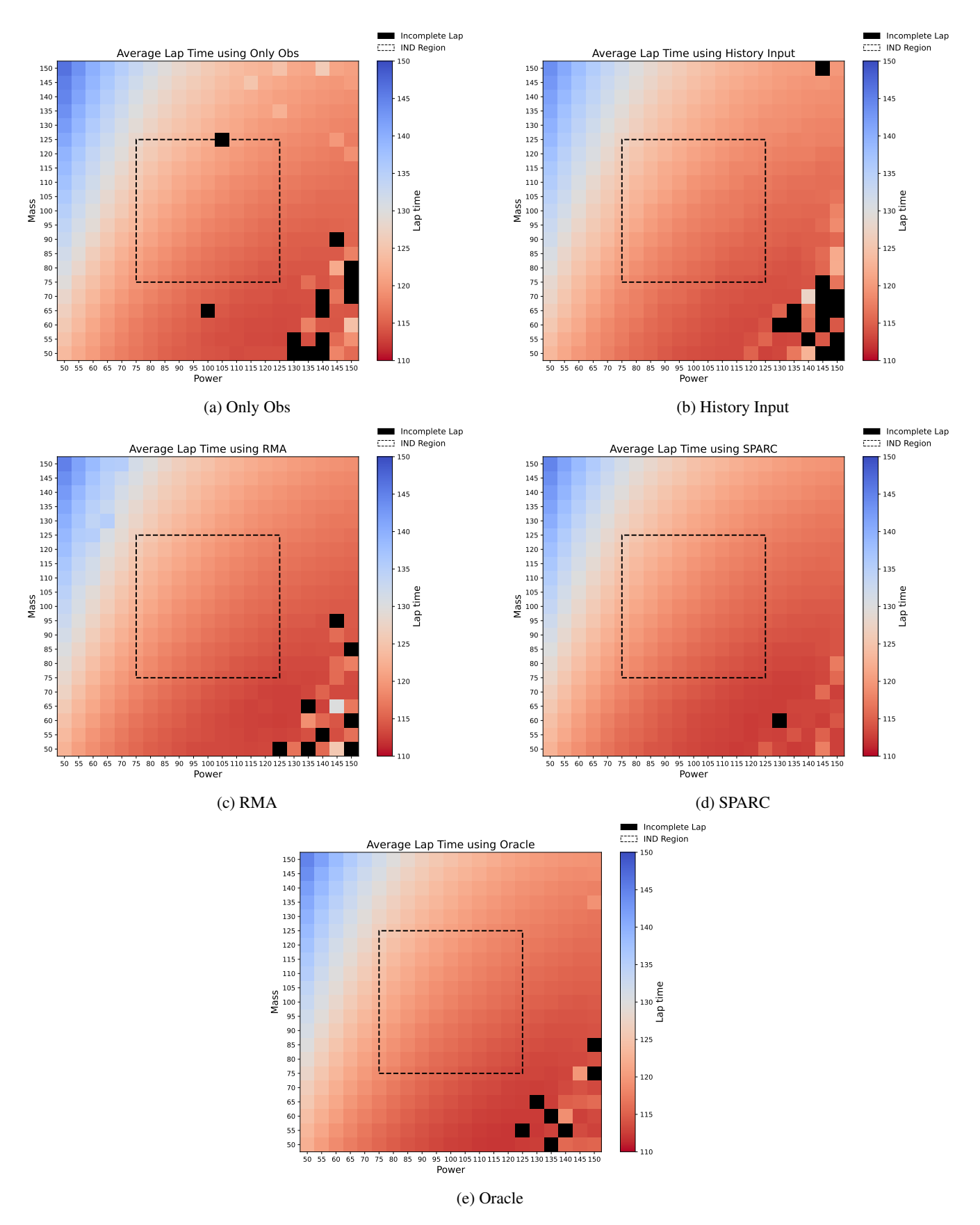


Figure 12: Lap times on the *Power & Mass* experiment. Colours denote average lap time (red = fast, blue = slow); black squares indicate at least one unfinished lap; the dashed box is the IND region. SPARC completes almost the entire grid and keeps lap times low even in the most extreme OOD settings, whereas other baselines either slow down notably or fail to finish.

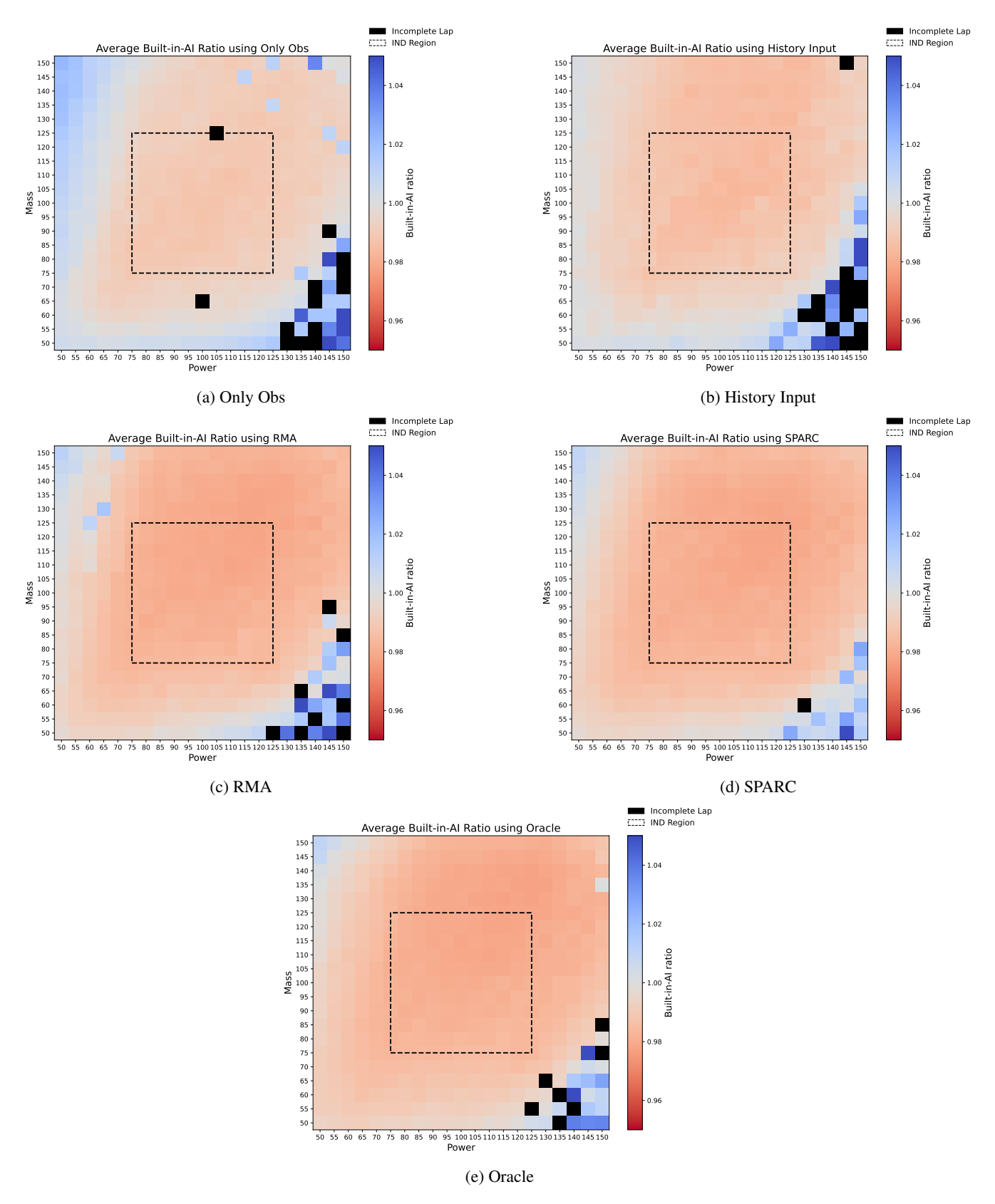


Figure 13: Built-in-AI ratios on the *Power & Mass* experiment. Normalising by the built-in AI removes the effect of absolute car speed; values above 1.0 (blue) indicate slower than the scripted driver. SPARC attains sub-BIAI lap times over the widest OOD area and shows the fewest non-completions, highlighting its superior adaptability.

C.3 MuJoCo Experiments

To probe fine-grained robustness in continuous-control domains, in Section 6.3 we add a horizontal (x) and vertical (z) wind force to every MuJoCo agent, as context within the environment. We present results of each baseline on all three environments (HalfCheetah-v5, Hopper-v5, Walker2d-v5) in Figures 15 to 17. Each heat-map cell shows the mean episode return over three seeds; darker red is higher reward, darker blue is lower. SPARC consistently matches or exceeds other baselines *inside* the dashed IND region and, crucially, maintains high returns as winds grow stronger.

The difference plot in Figure 14 makes an explicit comparison between the strong RMA baseline (Kumar et al. 2021) and SPARC. Most OOD cells are green (SPARC > RMA), confirming that the history adapter can indeed be trained simultaneously with the expert policy to generalise across a two-dimensional disturbance space.

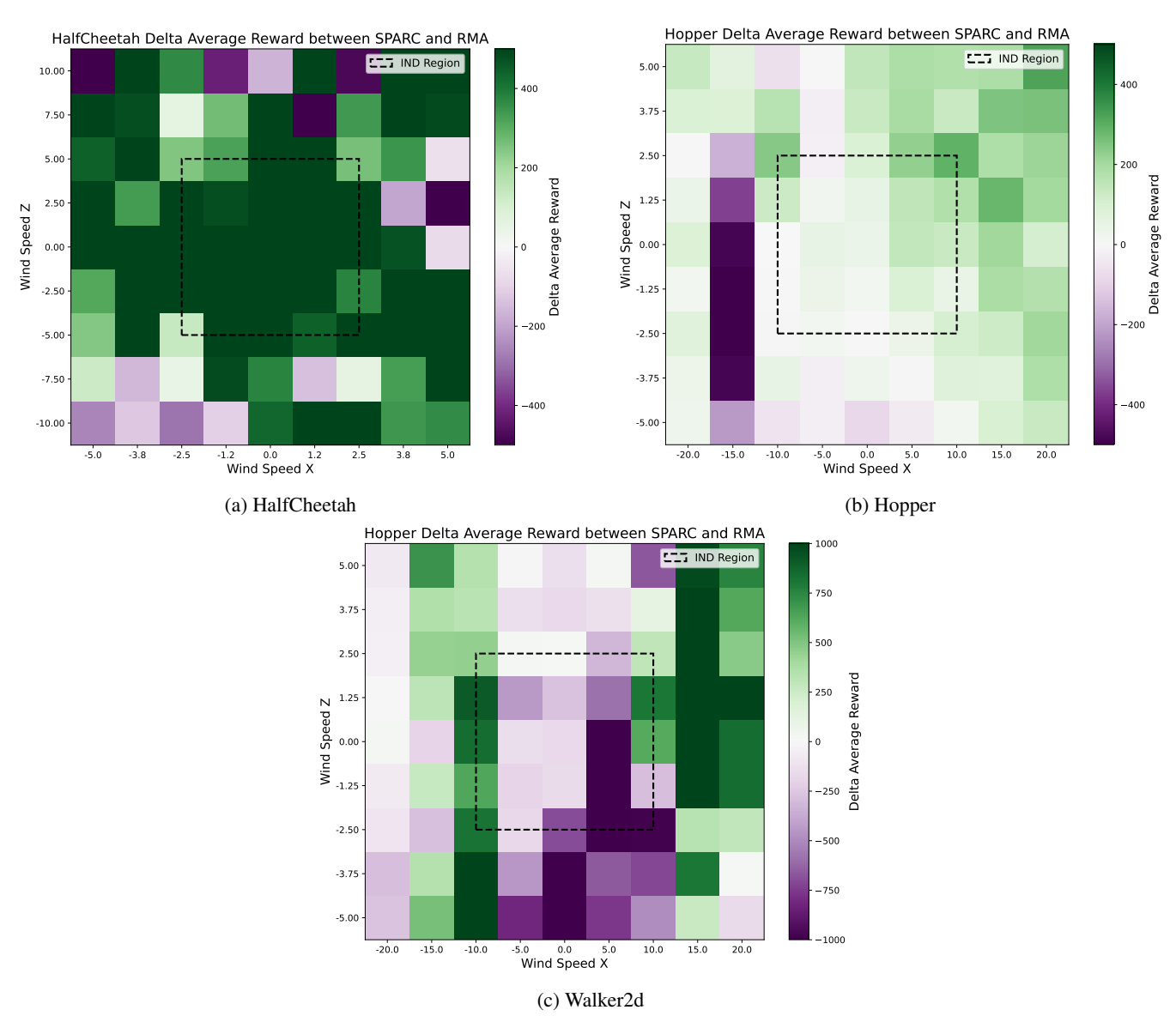


Figure 14: Delta average return of SPARC vs RMA for MuJoCo environments with different wind perturbations. In green: SPARC is better in that wind setting, while in purple: RMA scores higher. SPARC demonstrates a stronger robustness overall, especially in out-of-distribution contextual settings.

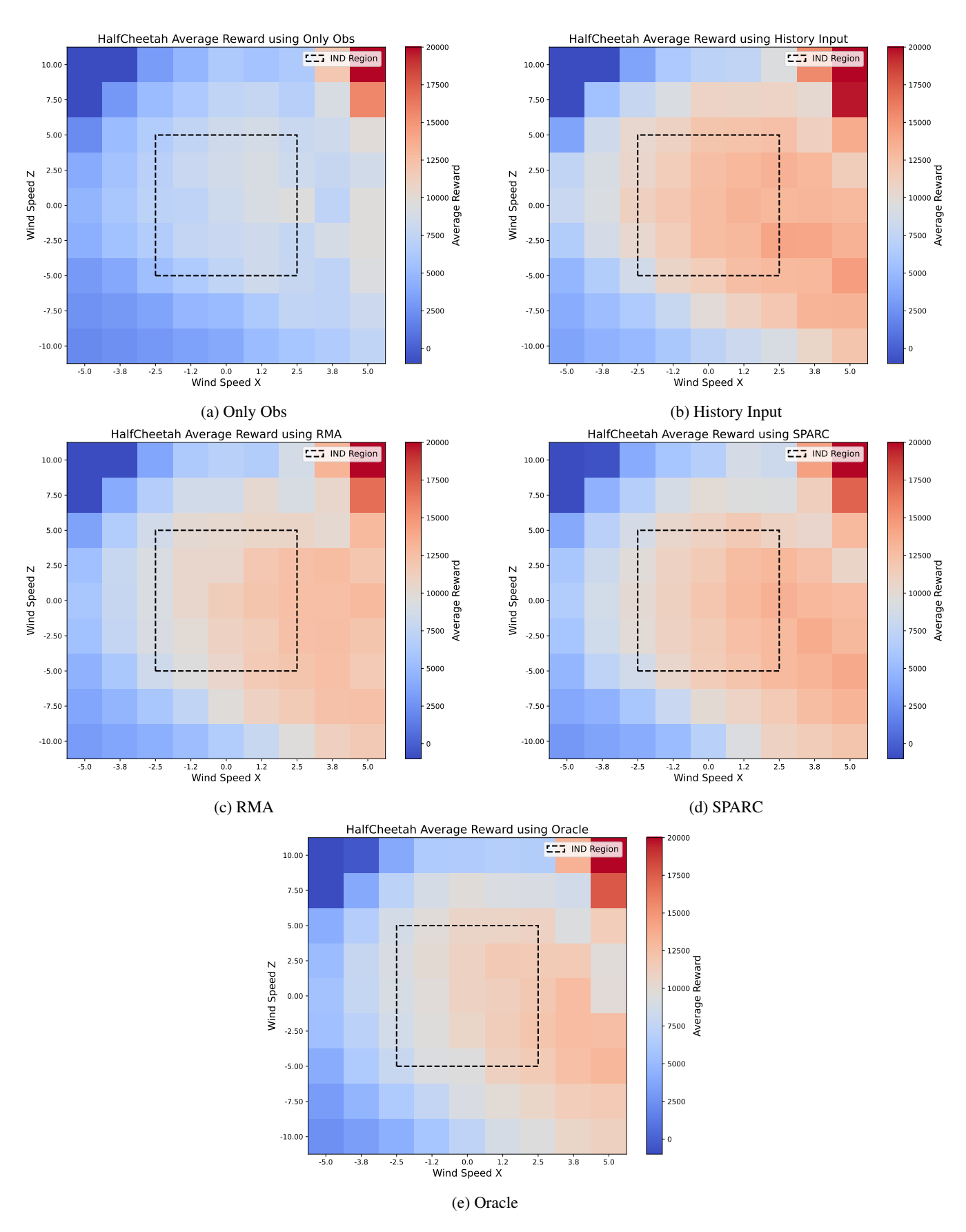


Figure 15: Average episode return of methods on **HalfCheetah-v5** with different wind perturbations (red is high reward, blue is low). SPARC retains near-Oracle performance throughout the grid.

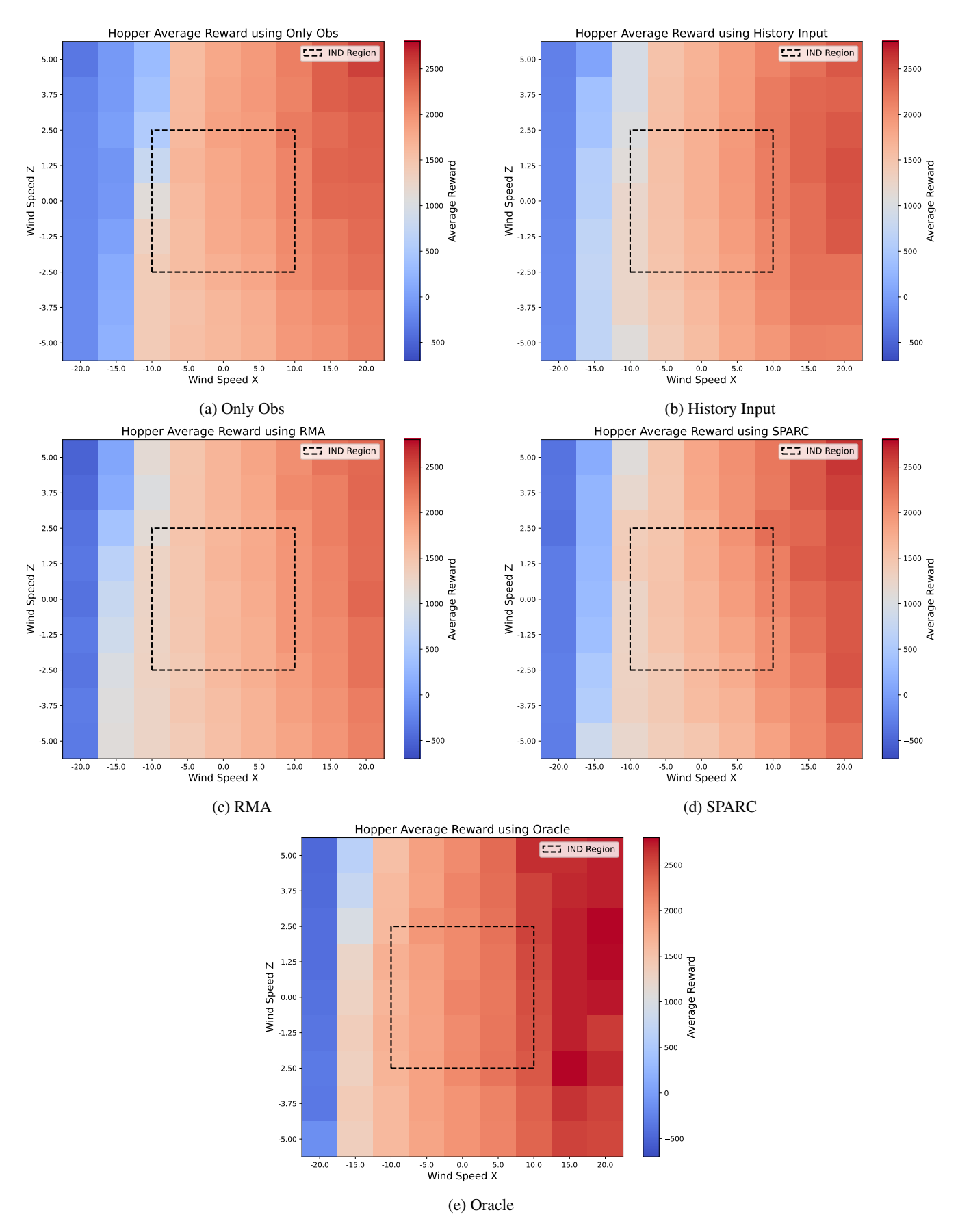


Figure 16: Average episode return of methods on **Hopper-v5** with different wind perturbations (red is high reward, blue is low). SPARC preserves stable hopping across almost the entire grid and outperforms RMA on most OOD cells (see also Figure 14).

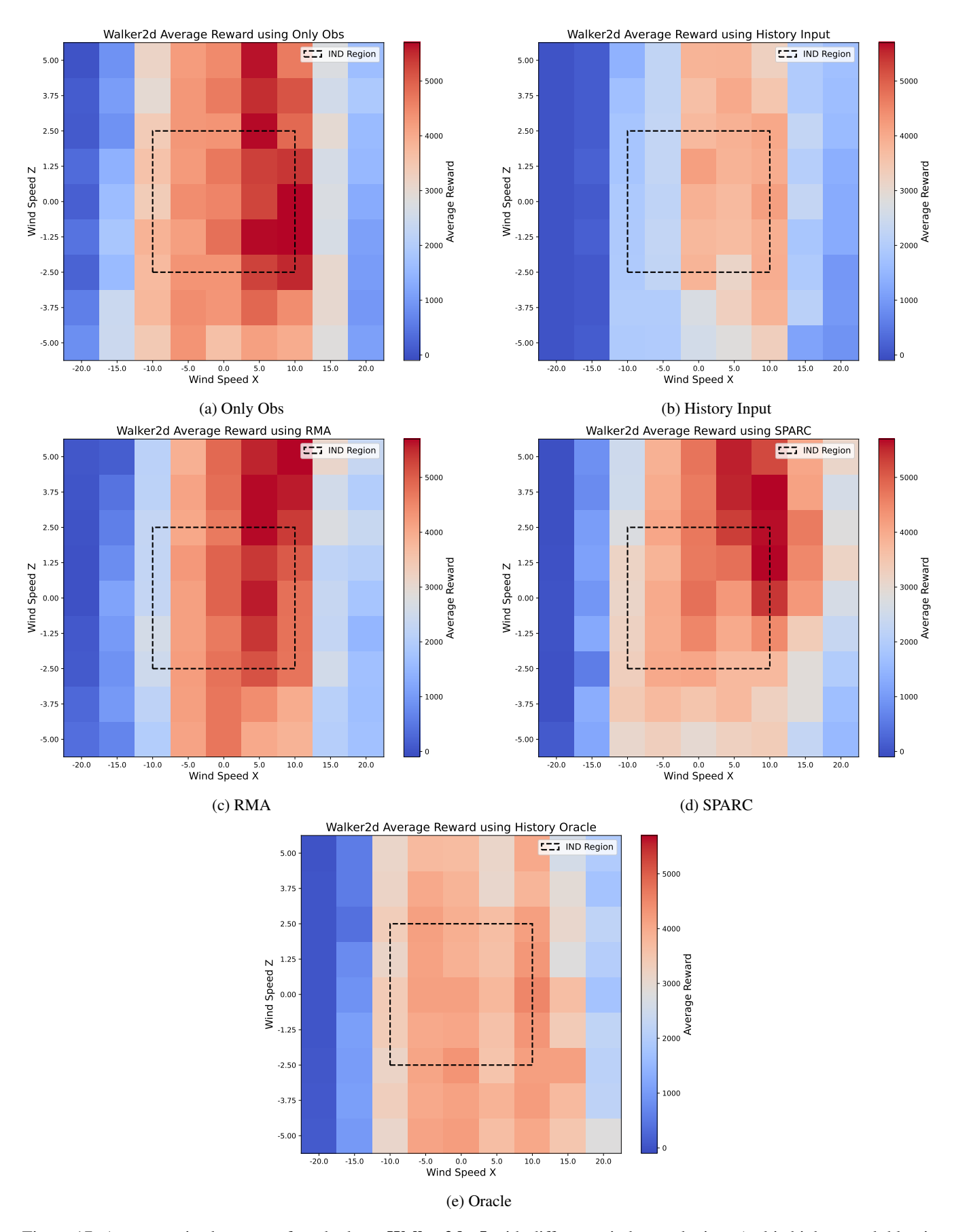


Figure 17: Average episode return of methods on **Walker2d-v5** with different wind perturbations (red is high reward, blue is low). Returns exhibit a characteristic ridge along positive x winds where the walker is pushed forwards. SPARC secures the highest rewards and records fewer falls than competing methods in many OOD settings.